

Fig. 2 Spherical earth correction on lateral range

"flat-earth" results also agree well with the spherical-earth results at higher $W/C_D A \rho$ if the initial velocity is low. At higher initial velocities and higher $W/C_D A \rho$, the spherical-earth correction becomes significant and causes a maximum lateral range to exist at a given initial velocity.

The question of what is the criterion for determining the significance of the lateral centrifugal force on lateral range has been discussed in Refs. 3 and 4 for the case of equilibrium glide. For an equilibrium glide, London⁴ advanced an argument that seems to apply also in the case of the constant-altitude glide. He indicated that the proper criterion for determining the validity of neglecting the lateral centrifugal force is the magnitude of the time integral of the ratio of this force to the lateral aerodynamic force, whereas the magnitude of the lateral range is not in itself a sufficient criterion. This seems to explain the characteristics of this correction noted previously. For a given initial velocity, the lateral aerodynamic force is large when $W/C_D A \rho$ is low, as can be seen from Eqs. (2) and (3). As a result, the lateral centrifugal force is never significant compared to the lateral aerodynamic force when $W/C_D A \rho$ is low and the correction is negligible. Equation (3) also shows that the lateral centrifugal force is approximately proportional to $\tan \lambda$, and consequently this force does not change appreciably for equal lateral range. For equal lateral range, therefore, the lateral-centrifugal-force correction should become larger at higher $W/C_D A \rho$ because the lateral aerodynamic force is lower, whereas the lateral centrifugal force stays relatively constant. This feature is shown clearly for the cases of high initial velocities of Fig. 1. A summary of the lateral-centrifugal-force correction is shown in Fig. 2.

The discussion presented in this note is for $L/D = 2$. Similar characteristics, although not shown here, have been observed for $L/D = 0.5, 1.0, 1.5$, and 2.5 . The foregoing findings can be summarized as follows:

- 1) The lateral range obtained during a constant-altitude glide over a spherical earth varies with $W/C_D A \rho$ and exhibits a maximum for a given initial velocity.
- 2) The spherical-earth correction is negligible at low $W/C_D A \rho$, regardless of the magnitude of lateral range and initial velocity, and becomes significant at high $W/C_D A \rho$ and high initial velocities.
- 3) The criterion for determining the significance of the lateral centrifugal force on lateral range seems to be the rela-

tive magnitude of the time integral of this force to the lateral aerodynamic force. This agrees with London's observation in the case of equilibrium glide.

References

- ¹ Skulsky, R. S., "Study of a particular lateral-range re-entry maneuver," TM 1364-61-16, Martin Co., Denver, Colo. (August 1961).
- ² Slye, R. E., "An analytical method for studying the lateral motion of atmosphere entry vehicles," NASA TN D-325 (September 1960).
- ³ Jackson, W. S., "An improved method for determining the lateral range of a gliding entry vehicle," J. Aerospace Sci. 28, 910 (1961).
- ⁴ London, H. S., "Comment on lateral range during equilibrium glide," J. Aerospace Sci. 29, 610 (1962).
- ⁵ London, H. S., "Change of satellite orbit plane by aerodynamic maneuvering," J. Aerospace Sci. 29, 323 (1962).

Forces due to the Magnetic Field of the Electrical Conductivity Meter

A. E. FUHS* AND R. BETCHOV†

Aerospace Corporation, Los Angeles, Calif.

A CONDUCTOR moving through an applied magnetic field causes induced currents. The magnitude of the induced magnetic field is a measure of the product of the electrical conductivity σ and velocity u of the conductor. An instrument to measure σu was flown aboard a re-entry vehicle.^{1, 2} The interaction of the moving conductor with the applied magnetic field also produces a force on the magnet; this force is a desirable effect for magnetoaerodynamic attitude control. However, for plasma-sheath measurement, the force is undesirable since it eventually could perturb the trajectory of the re-entry vehicle. The theory predicts a rather small force, but it is of interest to measure the force directly on the σu transducer for conditions simulating flight.

The x component of the force on the magnet is

$$F_x = \int_y \sigma(y) U(y) \int_x \int_z [B_z^2(x, y, z) + B_y^2(x, y, z)] dx dy dz \quad (1)$$

A right-handed coordinate system has been chosen with the x axis parallel to the flow and the y axis normal to the surface. The electric field is negligible (see Ref. 2) and, hence, has been neglected in the derivation of Eq. (1). The magnetic field B is proportional to the current in the primary coils i . Equation (1) shows that F_x is proportional to σ , to u , and to i^2 .

The components of the magnetic field of the flight transducer were measured with an aluminum plate covering the transducer. The aluminum plate duplicates the skin of the re-entry vehicle. To simulate the plasma flow, a spinning graphite disk was employed. Using the measured B_y and B_z and values of σ and u appropriate for the graphite disk, Eq. (1) was evaluated numerically. The results are shown in Fig. 1.

The force was determined experimentally using apparatus shown schematically in Fig. 2. Thin metal strips formed the hinges of a parallelogram suspension. Displacements, the order of 0.001 in., were determined by a differential transformer. The apparatus was adapted from a previous ex-

Received by IAS October 29, 1962; revision received December 3, 1962. O. L. Gibb contributed efficiently and effectively to the experimental aspects of the force-measuring program.

* Staff Scientist, Plasma Research Laboratory.

† Department Head, Plasma Research Laboratory.

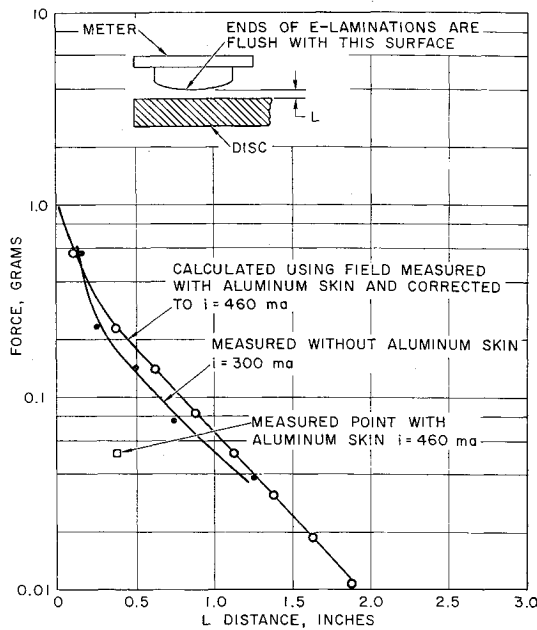


Fig. 1 Force as a function of the distance between the meter and the graphite disk

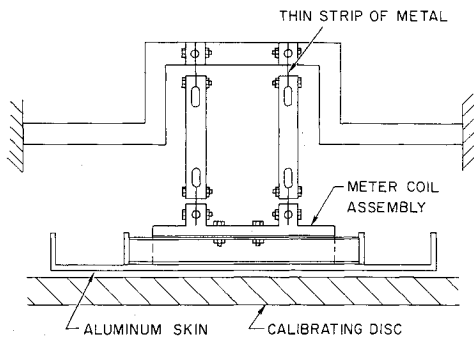


Fig. 2 A displacement parallel to the disk caused by the force on the coils

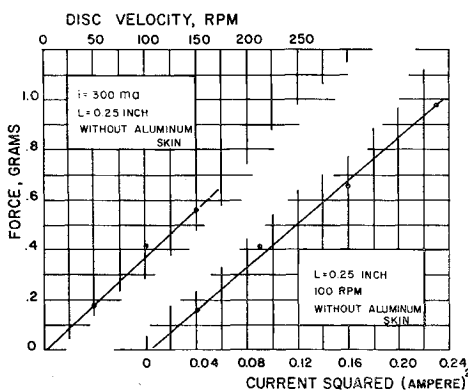


Fig. 3. Linear variation of force with velocity and with the square of the current in the primary coils

periment.³ Results of the measurement are shown in Fig. 1. The calculated and measured forces ($i = 460$ ma with aluminum skin) agree within a factor of 4. The calculated force and measured force curves show nearly identical slopes.

The predicted dependence of the force on u and i^2 shows excellent agreement with the experimentally determined dependence, as can be seen in Fig. 3. The force on the meter in flight would have been approximately 0.006 g. Thus, the presence of a conductivity meter is very unlikely to perturb the trajectory of the re-entry vehicle.

References

¹ Fuhs, A. E., "Development of a device for measuring electrical conductivity of ionized air during re-entry," Physical Research Lab., Space Technology Labs. Inc., STL/TR-60-0000-09256 (September 20, 1960).
² Betchov, R., Fuhs, A. E., Meyer, R. X., and Schaffer, A. B., "Measurement of electrical conductivity of ionized air during re-entry," Physical Research Lab., Aerospace Corp. Rept. TDR-594(1215-01)TR-1 (July 10, 1961); also Aerospace Eng. 21, 54-55, 68-78 (November 1962).
³ Schaffer, A. B., "Experimental study of an airfoil with a boundary layer subjected to magnetoaerodynamic forces," Physical Research Lab., Space Technology Labs. Inc., STL/TR-60-0000-09104 (May 3, 1960).

Behavior of a Trailing Vortex in a Favorable Pressure Gradient

JOHN E. GIBBONS* AND ERIK MOLLO-CHRISTENSEN†
 Massachusetts Institute of Technology, Cambridge, Mass.

The purpose of this study is the investigation of a streamwise vortex in low-turbulence channel flow, with particular attention to the high-shear region of the vortex core. Transverse-velocity profiles through the flow indicate that nearly discrete cylindrical vortex sheets are formed.

THE study is confined to vorticity in channel flow because of the relative simplicity of instrumenting the channel. The wind tunnel consisted of a settling chamber and a $3 \times 3 \times 27$ -in. test section with a free-jet exhaust. With an area ratio of 24:1 between settling chamber and test section, the turbulence level was held to an upper limit of 0.06%. The tunnel was driven from the downstream end to a maximum speed of 16 fps.

The vorticity was produced by the following arrangement. Two flat-plate wings at equal but opposite angles of attack were inserted into the flow from opposite sides of the test section, with provision for adjusting tip separation and angles of attack. The resulting tip vortices were forced together by the pressure field to produce a flow that is physically indistinguishable from a single vortex. (This statement was tested successfully by comparing velocity profiles through the vortex in the xy and xz planes.) The wing-tip separation was 0.125 in. and thus of the order of the boundary layer thickness at the wing trailing edge. During the test the Reynolds number based on wing chord lay in the range of 2000 to 17,000.¹

Velocity profiles across the test section were obtained by means of a hot-wire anemometer mounted on a sting downstream of the wing tips. The hot wire was held in alignment with a radius of the vortex, so that true absolute value of the velocity vector was measured, and errors due to the inherent directional sensitivity of the instrument were avoided. (This explains the velocity peak just outside the core in Fig. 1c.)

Results

Typical results of velocity-profile measurements are shown in Fig. 1. The profiles of absolute steady-state velocity $u(r, x)$ are shown for several streamwise distances x (measured downstream from the wing trailing edges) and for several values of uniform flow speed $U(x)$ outside the vortex.

Received by IAS October 31, 1962; revision received November 26, 1962.

* Student.

† Professor of Aeronautics and Astronautics.

¹ Gibbons, J. E., "Vortex bursting in swirl flow," S.B. Thesis, Mass. Inst. Tech. (1962).